



Research paper

3D Finite element model of a blast load in a tunnel

Giovanni Leonardi¹, Rocco Palamara², Federica Suraci³

Abstract: This paper presents a 3D finite element analysis of the effect caused by a blast inside a reinforced concrete tunnel. The simulated explosion was caused by the crash of a heavy vehicle transporting inflammable material (LPG). The finite element technique was used to analyze the structural problems on the tunnel reinforced concrete structure considering the fire action and the subsequent explosion (blast) effect, incorporating appropriate material models.

Through FEM software the tunnel behavior was described with regard to structural safety. Indeed, tunnels must be designed to withstand damage factors, so it is desirable that if such an explosion did occur, the tunnel should be able to return to service in safety as soon as possible with minor repairs. Therefore, following the presented analysis, the most important factors influencing the dynamic response and the damage of the structure could be identified. The simulation involved aspects of thermal analysis and structural problems and the tensions in the structure generated by the effect of temperature caused by the fire and by the blast overpressure were analyzed. Following this approach, the most important factors influencing the dynamic response and damage of structure can be identified and appropriate preventive measures can be designated.

Keywords: tunnel, explosion, blast, finite element analysis

¹Prof., PhD., Eng., Department of Civil, Energy, Environmental and Materials Engineering, University of Reggio Calabria, Via Graziella, Reggio Calabria, Italy, e-mail: giovanni.leonardi@unirc.it, ORCID: 0000-0002-6359-4489

²PhD., Eng., Department of Civil, Energy, Environmental and Materials Engineering, University of Reggio Calabria, Via Graziella, Reggio Calabria, Italy, e-mail: rocco.palamara@unirc.it, ORCID: 0000-0003-2898-9773

³PhD., Eng., Department of Civil, Energy, Environmental and Materials Engineering, University of Reggio Calabria, Via Graziella, Reggio Calabria, Italy, e-mail: federica.suraci@unirc.it, ORCID: 0000-0003-0215-6861

1. Introduction

Underground transit tunnel systems have a fundamental role in many countries, considering the cities expansion, the morphology of each area, and the significant increase of subways for public transportation. Indeed, the underground infrastructures provide a quick and cost-effective alternative to surface rails and roads for users. Tunnels must be designed to withstand damage factors, not only because of the user safety, but also because of transport network interruptions would cause considerable financial implications, in particular if the considered tunnel is part of a transport lifeline [1].

Among external damage factors, the blast is one of most dangerous for its unpredictability. So, it is essential that if such an explosion did occur, the tunnel should be able to return to service in safety as soon as possible with minor repairs, therefore transportation tunnels must be designed to mitigate the adverse effects of credible blast events.

One of the main dangerous cause of tunnel blast is the crash of heavy vehicles transporting inflammable material. In Europe, the road transportation volume of hazardous materials (HAZMAT) varies from 4% to 8% compared to the total transportation of European wares. In case of a heavy vehicle crash inside a tunnel, the possible container rupture could produce a fire, a consequent substantial blast and, obviously, the blast wave reflects repeatedly because of the limit of tunnel wall, its close-in effect makes the over pressure of tunnel blast wave increase and continuance time of the blast wave longer [2].

Blast phenomena in tunnel system have been the subject of many studies. Several authors have focused on the mechanical effects of an explosion on the structure of the tunnels whereas a few have presented the behavior of the blast wave in the tunnel. Van den Berg et al. [3] examined the blast effects originating from the rupture of a pressure tank in an urban tunnel system by a numerical simulation. The results, considering the tunnel length and a second blast wave, showed that an open space in the tunnel section in which the incident occurred, did not limit the lethal effects on the other sections. Chang and Young [4] gave different expressions of the incident pressure wave depending on the explosive mass and the radial distance. Buonsanti and Leonardi [5,6] used a finite element method to describe the behavior of a tunnel submitted to the blast generated by the explosion of an LPG (liquefied petroleum gas) tank, coupling the thermal and mechanical aspects.

In literature, there exist few numerical studies investigating the dynamic and nonlinear response of tunnels subjected to the simultaneous actions of fire and blast, so this paper introduces a FEM – finite element modelling – to evaluate the dynamic and damage response of a road tunnel structure under fire and explosion load caused by the rupture of an LPG road tank.

2. Model description

2.1. Geometry and materials

The analyzed longitudinal section of a road tunnel is 150 m, whereas the geometry of the cross section is represented in Fig. 1. The model is composed by two parts: the soil around the

tunnel (schematized by a parallelepiped) and the tunnel shell in CLS. The tunnel is about 10 m below the ground surface.

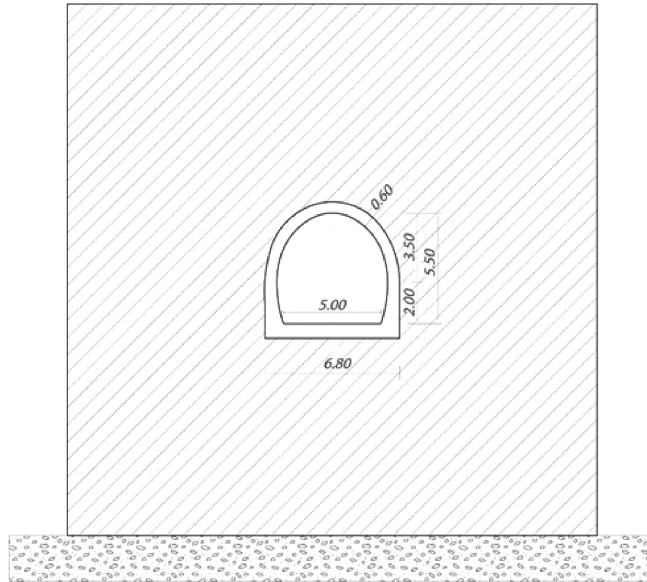


Fig. 1. Tunnel cross section

The soil behaviour was simulated using Drucker-Prager cap model in ABAQUS [7]. This model presents perfect plasticity as well as isotropic hardening. The soil properties obtained from [6, 8–10] are represented in Table 1.

Table 1. Drucker-Prager model parameters for soil

Parameter	Soil			
Density (kg/m^3)	1890			
Young's modulus E (MPa)	146.72			
Poisson's Ratio ν	0.20			
Material cohesion d (MPa)	1.38			
Material angle of friction β ($^\circ$)	37			
Initial cap yield surface position	0.02			
Transition surface radius parameter α	0.01			
Cap hardening behaviour:				
Stress (MPa)	2.75	4.14	5.51	6.20
Plastic volumetric strain	0.00	0.02	0.05	0.09
Specific Heat (J/kg K)	1840			
Thermal conductivity (W/m $^\circ\text{C}$)	2.00			

For the characterization of the reinforced concrete of the tunnel structure it was considered a C50/60 class concrete. The mechanical characteristics of the reinforced concrete (at a temperature of 20°C) are reported in Table 2.

Table 2. Characteristics of concrete

Young's modulus E (MPa)	Density (kg/m ³)	Poisson's Ratio ν
30000	2300	0.18

The thermal properties that govern temperature dependent properties in concrete structures are influenced by the aggregate type, moisture content and composition of concrete mix.

Numerous test programs and studies have been conducted for characterizing thermal properties of concrete at elevated temperatures [11–16]. The effects of high temperature on the characteristics of reinforced concrete were considered in the model according with the indications of the Eurocode 2 part 1–2 (EN 1992-1-2) [17, 18]. In particular, the used values of the elasticity modulus in function of temperature are reported in Table 3.

Table 3. Temperature dependence of concrete modulus of elasticity [19]

Temperature (°C)	20	50	200	400	600
Young's modulus E (MPa)	30000	30000	15000	4500	1500

EN 1992-1-2 provides the following simplifications to calculate the specific heat capacity and the thermal conductivity of concrete:

- the specific heat capacity is simply modeled by the following equation:

$$(2.1) \quad C_c(\theta) = 900 + 80 \left(\frac{\theta}{120} \right) - 4 \left(\frac{\theta}{120} \right)^2 \quad (\text{J/kg } ^\circ\text{C})$$

$$(2.2) \quad \lambda_c(\theta) = 1.5 - 0.26 \left(\frac{\theta}{120} \right) + 0.017 \left(\frac{\theta}{120} \right)^2 \quad (\text{W/m } ^\circ\text{C})$$

where: θ – temperature.

EN 1992-1-2 settles that the impact of reinforcement steel on the temperature distribution within concrete elements has not to be considered. In the literature there are numerous analytical constitutive models suggested for concrete material.

In this study the “Concrete Damaged Plasticity Model (CDPM)” was used. The CDPM requires concrete compressive and tensile constitutive relationship cracking and crushing damage parameters and special parameters such as dilation angle, eccentricity, biaxial loading ratio (f_{b0}/f_c), the coefficient K_c and viscosity parameter [8]. These parameters can be assigned to their commonly used values in the literature [20–22] (Table 4 and Table 5).

Table 4. The material parameters of CDP model for concrete class B50

Parameters of CDP model	Dilation Angle	Eccentricity	Initial uniaxial/biaxial ratio
	$\beta = 31^\circ$	$m = 0.1$	$f = f_{b0}/f_c = 3.0$

Table 5. Concrete damage parameters

Concrete compression hardening		Concrete compression damage	
Stress (MPa)	Crushing strain	Damage	Crushing strain
15.0	0.0	0.0	0.0
20.197804	0.0000747307	0.0	0.0000747307
30.000609	0.0000988479	0.0	0.0000988479
40.303781	0.000154123	0.0	0.000154123
50.007692	0.000761538	0.0	0.000761538
40.236090	0.002557559	0.195402	0.002557559
20.236090	0.005675431	0.596382	0.005675431
5.257557	0.011733119	0.894865	0.011733119
Concrete tension stiffening		Concrete tension damage	
Stress (MPa)	Cracking strain	Damage	Cracking strain
1.99893	0.0	0.0	0.0
2.84200	0.00003333	0.0	0.00003333
1.86981	0.000160427	0.406411	0.000160427
0.862723	0.000279763	0.69638	0.000279763
0.226254	0.000684593	0.920389	0.000684593
0.056576	0.00108673	0.980093	0.00108673

The influence of high temperatures on f_{b0}/f_c and K_c parameters was studied by researchers [23, 24] who found that the value of f_{b0}/f_c at ambient temperature is in the range of 1.1–1.3, while 2.0–3.0 for temperature 600°C and above. The considered maximum temperature in the tunnel fire is 1350°C so a constant value of 3.0 was used for the analysis. The K_c parameter is less temperature dependent, with values in the range of 0.6–0.67. The Abaqus default value of $K_c = 2/3$ was used in this analysis [23]. Eccentricity is a plastic flow potential parameter that describe the rate at which the function reach asymptote. The default value of 0.1 was used, indicating that the concrete has a dilation angle which almost similar over a wide range of stress values.

The viscosity parameter is for visco-plastic regularization of the concrete constitutive equations, a technique to overcome convergence difficulties. Smaller values of viscosity could produce more accurate results; however, smaller significantly increases the analysis time and is more prone to convergence problems. For this study, the value of the chosen viscous parameter is 0.00001 [25].

3. Methodology

The consequence of a catastrophic rupture of a pressure vessel of LPG is a boiling liquid expanding vapour explosion (BLEVE), which could produce a substantial blast action. This one can be decomposed in two components: thermal and shock wave loads. Consequentially

the analysis of fire resistance is an important aspect in the study of tunnel design. Several researches have taken place in both real, disused tunnels and laboratory conditions [10,26–30]. The data obtained from these tests have used to determine the impact of fire on structures using time-temperature curves. These temperature curves form the basis for developing requirements for tunnel construction, such as the thickness of the fire-protection cladding and the design of the escape and rescue strategies in the event of fire. The aim of these specifications is to protect the tunnel structure from excessive temperatures in the event of fire. The time-temperature curves differ in terms of fire development, the time before the maximum temperature is reached and the duration of impact of the maximum temperature. The internationally recognized time-temperature curves are summarized below and showed in Fig. 2.

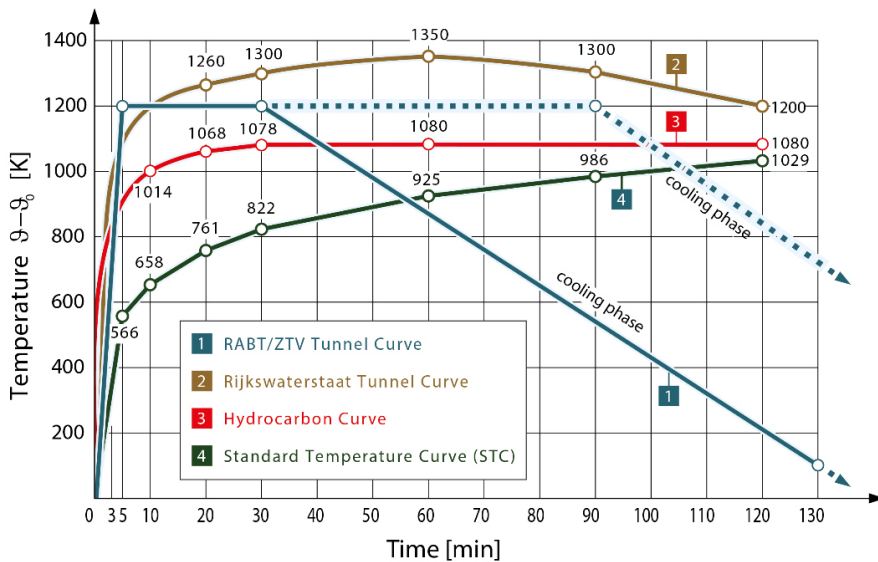


Fig. 2. Time-temperature curves [11, 12]

In this paper, a fire scenario according to the RWS curve was used to simulate the fire action inside the tunnel. The RWS curve was developed by the Rijkswaterstaat, Ministry of Transport in the Netherlands. This curve assumes that, in a worst-case scenario, a 50 m² fuel, oil or petrol tank fire with a fire load of 300 MW could occur, lasting up to 120 minutes. The RWS curve was based on laboratory scale tunnel tests performed by TNO in the Netherlands in 1979 [31]. The correctness of the RWS fire curve as a design fire curve for road tunnels was reconfirmed in the Full-Scale Tests in the Runehamar tunnel in Norway. According to the Runehamar tunnel fire tests [30], a typical commodity found in HGVs trailers could produce a rapidly growing fire producing a peak heat release rate of 200 MW [32]. Further, the measured maximum excess gas temperatures beneath the ceiling were approximately 1350°C. Considering this type of vehicular fire, the time history of heat fluxes (solid) shown below in Fig. 3 was considered in the numerical simulation.

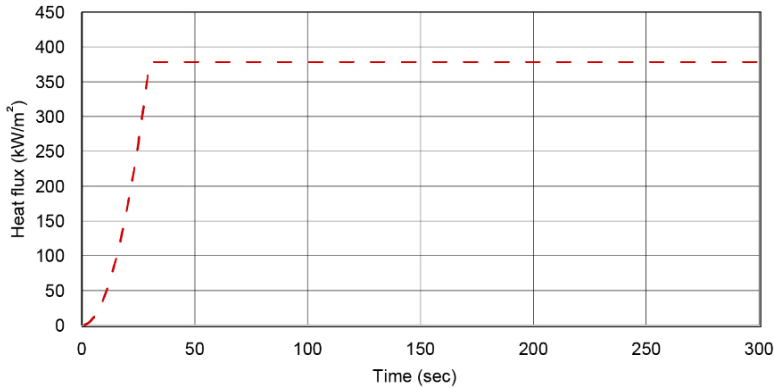


Fig. 3. Heat flux time history [33]

3.1. Blast-wave in tunnels

The effects of a road accident with a HAZMAT tank could be aggravated when it happens in built environments, such as urban areas or in partially confined spaces like tunnels. In fact, the effects of the BLEVE - boiling liquid expanding vapor explosion – of an LPG road tanker in an urban area accident become catastrophic for road users and first responders, when it occurs in a long tunnel where the gas expansion is not freely allowed and the blast-wave decays slowly.

A BLEVE is the explosive evaporation process as a consequence of the rupture of a pressure vessel containing a liquefied gas. Initially, the temperature of the liquid exceeds the boiling point under ambient conditions. The pressure in the vessel is equal to the vapor pressure at the liquid temperature. When the vessel ruptures, the pressure in the liquid falls and a superheated liquid remains. The subsequent flash evaporation process requires heat, which is extracted from the liquid. The evaporation process continues until the liquid temperature has fallen to the boiling temperature under ambient pressure.

Several studies [25, 34–37] have carried out the evaluation of the explosion effects inside the underground structures, focusing on the available energy converted into a blast-wave when an explosion occurred. In particular, the researches have shown the dependence of the peak overpressure with the distance from the explosion center, with the charge weight of course, and with the volume of tunnel segment. Silvestrini et al. [37] have introduced a factor (Energy Concentration Factor – ECF) that considers the spatial density of blast energy allows the evaluation of the peak side-on overpressure of blast-waves in partially confined geometries. The ECF is the ratio between volume of the hemisphere with radius r_0 and volume of the confined region included in the distance r_0 from the epicenter of blast [38]. With a reference to a tunnel in which the explosion is occurred at the center of a tunnel, the ECF is as follows:

$$(3.1) \quad \text{ECF} = \frac{V_{H\text{Sph}}}{V_{\text{Tun}}} = \frac{\frac{2}{3}\pi r_0^3}{2Ar_0} = \frac{1}{3} \frac{\pi}{A} r_0^2$$

where: A is the tunnel cross sectional area

The Energy Concentration Factor is a purely geometrical factor that considers the increase in spatial density of energy caused by the reduction of the volume available for gas expansion.

The evaluation of the peak side-on overpressure developed at different locations from the blast source can be done using the Sachs scaled distance, via change of the scaled with ECF. When a BLEVE occurs in open environment, the peak side-on overpressure of the blast wave is normally evaluated by means of scaled over pressure curves [34] that provide the scaled overpressure (P_S/P_0) as function of the Sachs scaled distance. This last one is given by the following expression:

$$(3.2) \quad \bar{R} = r_0 \left(\frac{P_0}{2W} \right)^{1/3}$$

where: r_0 [m] is the distance from the blast source, W [J] is the expansion work devoted to blast-wave generation and P_0 [Pa] is the atmospheric pressure.

The expansion work devoted to blast-wave generation W can be determined either with the method of Casal and Salla [39] or by means of empirical correlations such as that for propane proposed by Genova et al. [40]:

$$(3.3) \quad W = 182m(T + 42.09)$$

where: m [kg] is the mass of LPG in the road tanker and T [°C] is the temperature of LPG at the instant preceding the bursting of the tank.

The use of the Energy Concentration Factor leads to a modified expression of the Sachs scaled distance on the form:

$$(3.4) \quad \bar{R}' = r_0 \left(\frac{P_0}{2ECF \cdot W} \right)$$

The pressure P_S is obtained through \bar{R}' using the scaled overpressure distance shown in Fig. 4.

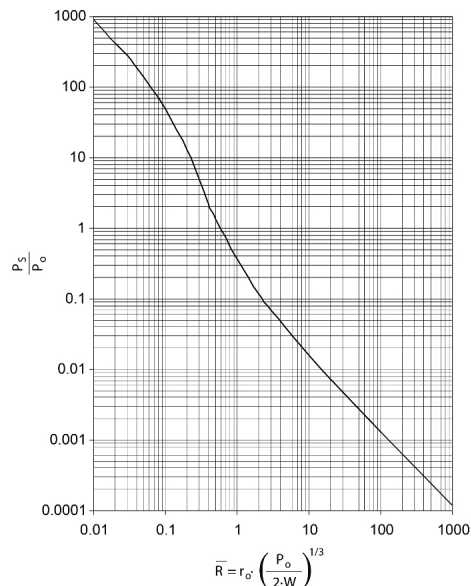


Fig. 4. Scaled overpressure distance

During the propagation of the blast wave over the first 75 m from the BLAVE to the tunnel opening, the blast overpressure falls from 1700 kPa (vapour pressure at 326 K) down to approximately 97 kPa (Table 6).

Table 6. Overpressure in a tunnel of 28 m² section area for the BLAVE of a 50 m³ LPG rail tanker

Distance (m)	50	100	150
ECF	87	349	785
R'	0.52	0.66	0.76
P_0/P_s	1.1	0.8	0.65
P_s (Pa)	111457	81060	65861

4. Model verification

This paragraph presents the finite element analysis of a road tunnel and in particular the description of the tunnel geometrical characteristics, its materials, the loads (fire and blast) in the space and time domains, the mesh model and the analysis results in terms of stress, strain and total deformation obtained by ABAQUS software.

The main aspect in this study is the combination of fire and blast loads. Moreover, the vertical load caused by 16 m of above ground soil is considered. The model geometry has been chosen to simulate the effects of the explosion according to several studies [41–44].

As stated above, the heat flux time history curve (Fig. 3) is used to simulate the fire action inside the road tunnel. According to Root [33], the longitudinal distribution of the incident heat flux on the top of the tunnel is illustrated in Fig. 5.

The blast overpressure is generated by the explosion of 50 m³ LPG tank occurred in the middle of the road tunnel. For this type of tanker, the vapor pressure is 1700 kPa at the moment

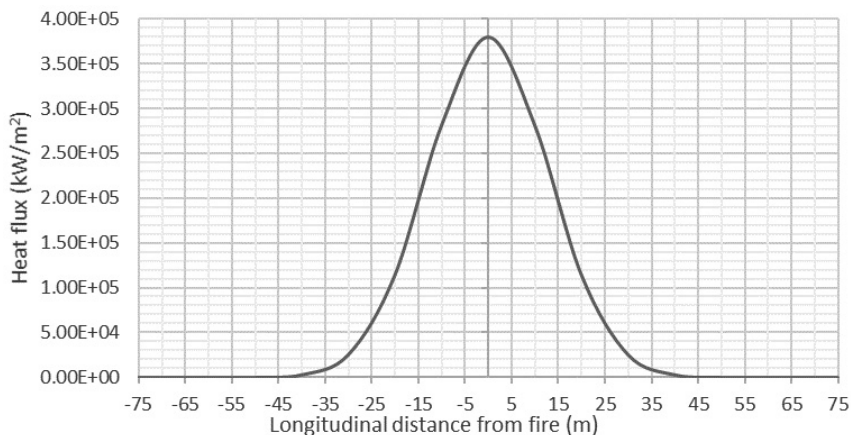


Fig. 5. Longitudinal (top) distribution of incident heat flux

of the explosion. Considering that the tunnel cross section area and the three main distances from the blast source are 0 m, 25 m, 75 m, it is possible to calculate the variation of P_S inside the structure by means of the Sachs scaled distance modified with Energy Concentration Factor – ECF, the results are shown in Table 6.

The pressure-time curve was assumed to be of triangular shape, the duration of which was obtained from CONWEB reflected pressure diagram [45].

The used mesh model for each part is represented by linear hexahedral elements of type C3D8HT obtaining 31980 elements and 36844 nodes. The mesh for tunnel shell has smaller dimensions than the mesh for soil in order to evaluate its response in a satisfactory manner (Fig. 6). The degree of mesh refinement is the most important factor in estimating an accurate stress field in the structure: the finest mesh is required near the loads to capture the stress and strain gradients.

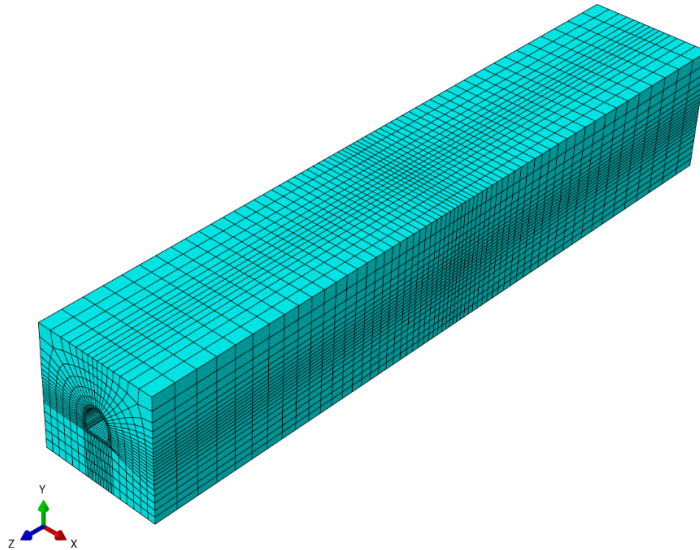


Fig. 6. Mesh model

The external solid is fixed at the base and its other sides have elastic supports to simulate the soil reaction. The analysis has been carried out in three steps. The first step obtained the initial stress state caused by fire, the second step analysed the dynamic response under blast loading, the last step simulated the fire load after the explosion. The explosion can occur after a few minutes from the start of the fire action, or even after a shorter time. In the San Juanico accident (Mexico, 1984), the first BLEVEs occurred 70 seconds after the first jet fires appeared [32]. Consequently, the following load conditions have been considered in the FE analysis:

- 1) from time $t = 0$ to $t = 70$ sec the tunnel was subjected to the fire thermal stress;
- 2) at the instant $t = 70$ sec the structure was subjected to the blast over pressure of 1700 kPa.
- 3) from time $t = 70$ sec to $t = 1870$ sec the tunnel continued to be subjected to the fire thermal stress.

4.1. Results and discussion

The initial stress state caused by fire action is obtained through the first step, whereas thanks to the second and the third steps, it is possible to analyze the dynamic response under blast loading.

Therefore, on the base of this analysis, the distribution of the temperature, after 70 sec, inside of the structure is known (Fig. 7).

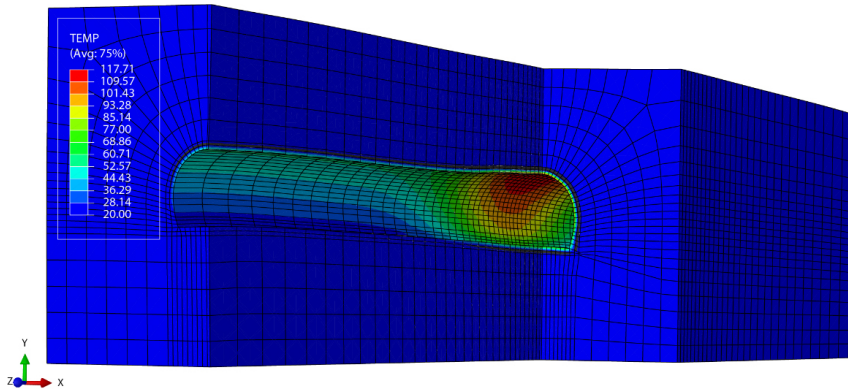


Fig. 7. Temperature distribution ($^{\circ}\text{C}$) at the instant before explosion ($t = 70$ sec)

In Fig. 8 the thermal plastic strain components at the same time ($t = 70$ sec) on the tunnel shell are showed.

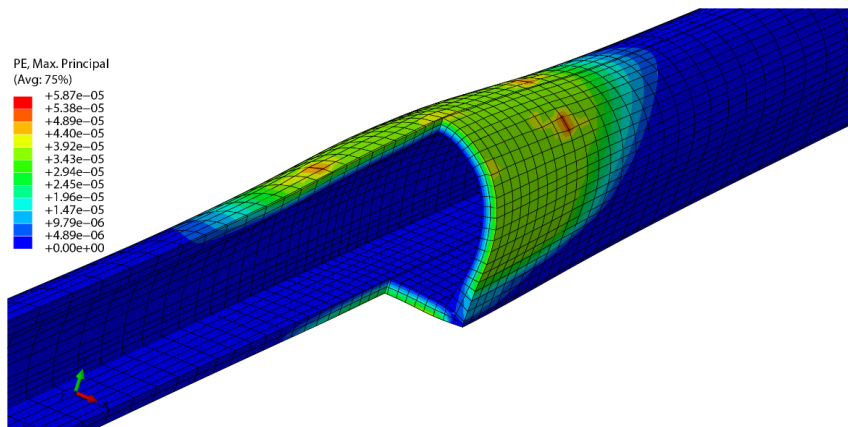


Fig. 8. Plastic strain components at the instant before explosion ($t = 70$ sec)

In these two figures the first important effects of the fire on the structure can be observed. Then, the mechanical behavior of the model was analyzed introducing also to thermal stress, the overpressure caused by explosion (Fig. 9).

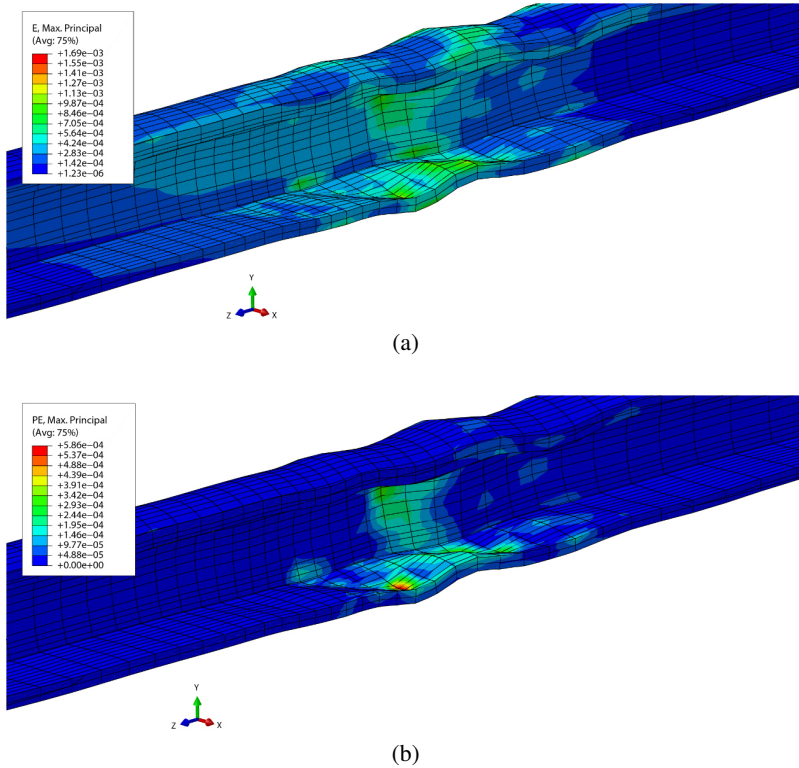


Fig. 9. Elastic strain components (a) and plastic strain components (b) after the explosion

Analyzing the results, it is clear that the deformation obtained in the middle of the tunnel is over the elasto-plastic limit and, consequently, it confirms a diffused fracture state for the CLS and a damage at the structure (Fig. 10). Plastic strain (Fig. 11) shows the extent of damage that the tunnel lining suffers due to the explosion and it is evident that the concrete suffers severe damage.

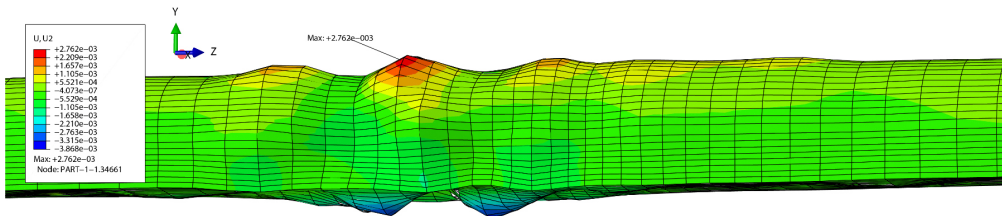


Fig. 10. Maximum vertical deformation at explosion time

In the last step of analysis (from $t = 70$ sec to $t = 1870$ seconds) the tunnel continued to be subjected to the fire thermal stress (Fig. 12).

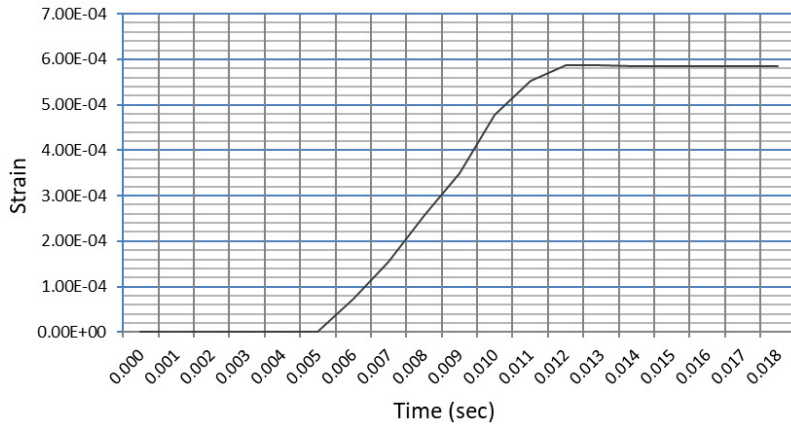


Fig. 11. Maximum principal plastic strain vs explosion time

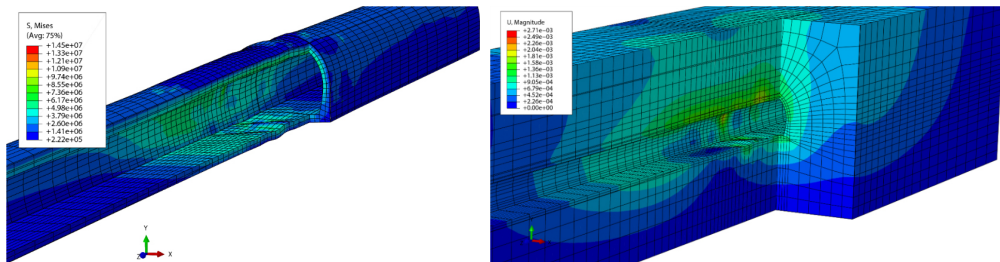


Fig. 12. Mises stress (Pa) and total deformation (m) at the simulation end

5. Conclusions

In this study a finite element analysis was carried out to investigate the consequences of a blast load on an underground transport infrastructure, considering the blast-wave through different overpressures in specific tunnel points and the variation of the fire action in the time domain. The proposed approach could be used to forecast the structure damage of existing subways and tunnels and to design new underground structures, considering that this type of analysis could be implemented studying, for example, the explosion at the end of the tunnel and, also, the variation of the temperature in the space, in order to consider the temperature gradient decrease.

References

- [1] F. Cirianni, G. Leonardi, and F. Scopelliti, "A methodology for assessing the seismic vulnerability of highway systems", in: AIP Conference Proceedings, vol. 1020, no. 1, American Institute of Physics, pp. 864–871, 2008, DOI: [10.1063/1.2963925](https://doi.org/10.1063/1.2963925).
- [2] J. Liu, Q. Yan, and J. Wu, "Analysis of blast wave propagation inside tunnel", Transactions of Tianjin University, vol. 14, no. 5, pp. 358–362, 2008, DOI: [10.1007/s12209-008-0061-3](https://doi.org/10.1007/s12209-008-0061-3).

- [3] A. Van den Berg, and J. Weerheijm, “Blast phenomena in urban tunnel systems”, *Journal of Loss Prevention in the Process Industries*, vol. 19, no. 6, pp. 598–603, 2006, DOI: [10.1016/j.jlp.2006.03.001](https://doi.org/10.1016/j.jlp.2006.03.001).
- [4] D.B. Chang and C.S. Young, “Probabilistic estimates of vulnerability to explosive overpressures and impulses”, *Journal of Physical Security*, vol. 4, no. 2, pp. 10–29, 2010.
- [5] M. Buonsanti, G. Leonardi, and F. Scopelliti, “3-D Simulation of shock waves generated by dense explosive in shell structures”, *Procedia Engineering*, vol. 10, pp. 1554–1559, 2011, DOI: [10.1016/j.proeng.2011.04.259](https://doi.org/10.1016/j.proeng.2011.04.259).
- [6] M. Buonsanti and G. Leonardi, “3-D simulation of tunnel structures under blast loading”, *Archives of Civil and Mechanical Engineering*, vol. 13, no. 1, pp. 128–134, 2013, DOI: [10.1016/j.acme.2012.09.002](https://doi.org/10.1016/j.acme.2012.09.002).
- [7] ABAQUS Inc., *ABAQUS Example Manual*, 2014.
- [8] ABAQUS Inc., *ABAQUS Theory Manual*, 2014.
- [9] ABAQUS Inc., *ABAQUS Analysis Manual*, 2014.
- [10] M. Nawar et al., “Numerical analysis of underground tunnels subjected to surface blast loads”, *Frattura ed Integrità Strutturale*, vol. 15, no. 55, pp. 159–173, 2020, DOI: [10.3221/IGF-ESIS.55.12](https://doi.org/10.3221/IGF-ESIS.55.12).
- [11] T. Lie and V. Kodur, “Thermal and mechanical properties of steel-fibre-reinforced concrete at elevated temperatures”, *Canadian Journal of Civil Engineering*, vol. 23, no. 2, pp. 511–517, 1996, DOI: [10.1139/196-055](https://doi.org/10.1139/196-055).
- [12] M.G. Van Geem, J. Gajda, and K. Dombrowski, “Thermal properties of commercially available high-strength concretes”, *Cement, Concrete and Aggregates*, vol. 19, no. 1, pp. 38–54, 1997, DOI: [10.1520/cca10020j](https://doi.org/10.1520/cca10020j).
- [13] V. Kodur and M. Sultan, “Effect of temperature on thermal properties of high-strength concrete”, *Journal of Materials in Civil Engineering*, vol. 15, no. 2, pp. 101–107, 2003, DOI: [10.1061/\(ASCE\)0899-1561\(2003\)15:2\(101\)](https://doi.org/10.1061/(ASCE)0899-1561(2003)15:2(101)).
- [14] V.K. Kodur, M. Dwaikat, and M. Dwaikat, “High-temperature properties of concrete for fire resistance modeling of structures”, *ACI Materials Journal*, vol. 105, no. 5, p. 517, 2008.
- [15] L. Guo, L. Guo, L. Zhong, and Y. Zhu, “Thermal conductivity and heat transfer coefficient of concrete”, *Journal of Wuhan University of Technology, Materials Science Edition*, vol. 26, no. 4, pp. 791–796, 2011, DOI: [10.1007/s11595-011-0312-3](https://doi.org/10.1007/s11595-011-0312-3).
- [16] V. Kodur, “Properties of concrete at elevated temperatures”, *International Scholarly Research Notices*, vol. 2014, 2014, DOI: [10.1155/2014/468510](https://doi.org/10.1155/2014/468510).
- [17] European Committee, “Eurocode2: Design of concrete structures-Part 1-2: General rules-Structural fire design”, *ENV 1992-1-2*, 1995.
- [18] J. Zehfuß et al., “Evaluation of Eurocode 2 approaches for thermal conductivity of concrete in case of fire”, *Civil Engineering Design*, vol. 2, no. 3, pp. 58–71, 2020.
- [19] UNI 9502:2001 – Analytical fire resistance assessment of reinforced concrete and prestressed concrete structural elements, UNI – Ente Nazionale Italiano di Unificazione, Milano, Italy, 2001.
- [20] T. Jankowiak and T. Lodygowski, “Identification of parameters of concrete damage plasticity constitutive model”, *Foundations of civil and environmental engineering*, vol. 6, no. 1, pp. 53–69, 2005.
- [21] J.S. Tyau, “Finite element modeling of reinforced concrete using 3-dimensional solid elements with discrete rebar”, (Master of Science), Brigham Young University, 2009.
- [22] Y. Dere and M.A. Koroglu, “Nonlinear FE modeling of reinforced concrete”, *International Journal of Structural and Civil Engineering Research*, vol. 6, no. 1, pp. 71–74, 2017.
- [23] F. Lo Monte, N. Kalaba, and P. Bamonte, “On the extension of a plastic-damage model to high temperature and fire”, in *IFireSS 2017-2nd International Fire Safety Symposium*, Doppiavoce, pp. 703–710, 2017.
- [24] N. Wahid, T. Stratford, and L. Bisby, “Calibration of concrete damage plasticity model parameters for high temperature modelling of reinforced concrete flat slabs in fire”, *Applications of Structural Fire Engineering*, Singapore, 2019.
- [25] A.S. Genikomsou and M.A. Polak, “Finite element analysis of punching shear of concrete slabs using damaged plasticity model in ABAQUS”, *Engineering Structures*, vol. 98, pp. 38–48, 2015, DOI: [10.1016/j.engstruct.2015.04.016](https://doi.org/10.1016/j.engstruct.2015.04.016).
- [26] Forschungsgesellschaft für Straßen – und Verkehrswesen, *Richtlinien für Ausstattung und Betrieb von Tunneln (RABT)*. Ausgabe, 1985.
- [27] M. Masellis, “Fire disaster in a motorway tunnel”, *Annals of Burns and Fire Disasters*, vol. 10, no. 4, pp. 233–240, 1997.

- [28] R.J. Proctor, "The San Fernando Tunnel explosion, California", *Engineering Geology*, vol. 67, no. 1–2, pp. 1–3, 2002.
- [29] S. Brambilla and D. Manca, "The viareggio LPG railway accident: event reconstruction and modelling", *Journal of Hazardous Materials*, vol. 182, no. 1–3, pp. 346–357, 2010, DOI: [10.1016/j.jhazmat.2010.06.039](https://doi.org/10.1016/j.jhazmat.2010.06.039).
- [30] H. Ingason, Y.Z. Li, and A. Lönnemark, "Runehamar tunnel fire tests", *Fire Safety Journal*, vol. 71, pp. 134–149, 2015.
- [31] Instituut TNO voor Bouwmaterialen en Bouwconstructies, Rapport betreffende de beproeving van het gedrag van twee isolatiematerialen ter bescherming van tunnels tegen brand (Rapport B-80-33). Delft, The Netherlands, 1980.
- [32] B. Hemmatian, E. Planas, and J. Casal, "Fire as a primary event of accident domino sequences: the case of BLEVE", *Reliability Engineering and System Safety*, vol. 139, pp. 141–148, 2015, DOI: [10.1016/j.res.2015.03.021](https://doi.org/10.1016/j.res.2015.03.021).
- [33] K.J. Root, "Development and verification of a confined discretized solid flame model for calculating heat flux on concrete tunnel liners", 2018.
- [34] H.R. Weibull, "Pressures recorded in partially closed chambers at explosion of TNT charges", *NYASA*, vol. 152, no. 1, pp. 357–361, 1968, DOI: [10.1111/j.1749-6632.1968.tb11987.x](https://doi.org/10.1111/j.1749-6632.1968.tb11987.x).
- [35] D.R. Curran, "Underground storage of ammunition: experiments concerning accidental detonation in an underground chamber", Norwegian Defence Construction Service, 1966.
- [36] A.C. Smith and M.J. Sapko, "Detonation wave propagation in underground mine entries", *Journal of the Mine Ventilation Society of South Africa*, vol. 58, pp. 20–25, 2005.
- [37] M. Silvestrini, B. Genova, and F. Leon Trujillo, "Energy concentration factor. A simple concept for the prediction of blast propagation in partially confined geometries", *Journal of Loss Prevention in the Process Industries*, vol. 22, no. 4, pp. 449–454, 2009, DOI: [10.1016/j.jlp.2009.02.018](https://doi.org/10.1016/j.jlp.2009.02.018).
- [38] Center for chemical process safety, Guidelines for Evaluating the Characteristics of Vapor Cloud Explosions, Flash Fires and BLEVEs. American Institute of Chemical Engineers, 1994.
- [39] J. Casal and J. M. Salla, "Using liquid superheating energy for a quick estimation of overpressure in BLEVEs and similar explosions", *Journal of Hazardous Materials*, vol. 137, no. 3, pp. 1321–1327, 2006, DOI: [10.1016/j.jhazmat.2006.05.001](https://doi.org/10.1016/j.jhazmat.2006.05.001).
- [40] B. Genova, M. Silvestrini, and F. L. Trujillo, "Evaluation of the blast-wave overpressure and fragments initial velocity for a BLEVE event via empirical correlations derived by a simplified model of released energy", *Journal of Loss Prevention in the Process Industries*, vol. 21, no. 1, pp. 110–117, 2008, DOI: [10.1016/j.jlp.2007.11.004](https://doi.org/10.1016/j.jlp.2007.11.004).
- [41] S. Koneshwaran, "Blast response and sensitivity analysis of segmental tunnel", PhD Thesis, Queensland University of Technology, 2014.
- [42] R. Tiwari, T. Chakraborty, and V. Matsagar, "Dynamic analysis of underground tunnels subjected to internal blast loading", *World Congress of Computational Mechanics (WCCM XI)*, Barcelona, 2014.
- [43] S. Koneshwaran, D. Thambiratnam, and C. Gallage, "Performance of buried tunnels subjected to surface blast incorporating fluid-structure interaction", *Journal of Performance of Constructed Facilities*, 2015, DOI: [10.1061/\(ASCE\)CF.1943-5509.0000585](https://doi.org/10.1061/(ASCE)CF.1943-5509.0000585).
- [44] M. Zaid and R. Sadique, "The response of rock tunnel when subjected to blast loading: finite element analysis", *Engineering Reports*, 2021.
- [45] D. Hyde, "CONWEP, Conventional Weapons Effects Program", US Army Engineer Waterways Experiment Station, Vicksburg, MS, 1992.